Parametric Analysis of Crystal-field Effects in Rare-earth-metal Disilicates doped with Trivalent Europium

Christian Chateau
U.P.R. 211 du C.N.R.S., 1, Pl. A. Briand, F-92190 Meudon, France
Jorma Hölsä *
Department of Chemical Engineering, Helsinki University of Technology, SF-02150 Espoo, Finland
Pierre Porcher
U.P.R. 210 du C.N.R.S., 1, Pl. A. Briand, F-92190 Meudon, France

The u.v. and dye-laser excited luminescence spectra of the Eu^{3+}-doped rare-earth-metal disilicates C-$M_2Si_2O_7$ (M = Y, Lu, Sc, or In) were recorded at 77 and 300 K. The $^7F_{0-5}$ energy-level schemes of the Eu^{3+} ion derived from the spectral analysis were simulated with the aid of phenomenological crystal-field theory. The C_2 symmetry simulation with nine real and five imaginary parameters of the experimental crystal-field splittings of the energy levels was excellent with root mean square deviations varying between 4 and 6 cm^{-1}. The best-fit parameter values behave in a smooth manner as a function of the host cation in the structurally isomorphic disilicate series. The indium disilicate has slightly different values, however. The strength of the crystal-field effect decreases slightly with increasing ionic radius of the rare-earth-metal host. A comparison of the experimental parameter sets with those obtained for Eu^{3+}-doped rare-earth-metal oxysalts revealed fundamental differences.

The rare-earth-metal silicates constitute an important group of compounds due to their excellent stability against decomposition resulting in formation of minerals.[1] A great number of such silicate compounds is known indicating that their chemistry is not simple and straightforward, however. The most common silicates can be formed with the $M_2O_3:SiO_2$ ratios of 1:1, 2:3, and 1:2.[2] Within the main structural types there exists a variety of polymorphic forms the presence of which depends on the experimental conditions of preparation, *i.e.* the temperature and pressure used.[3-7] The bulk of these compounds known to date is already well characterized from the structural point of view. The natural minerals, thortveitite and thalenite, are among the best known rare-earth-metal silicates. Even the luminescence properties of such silicates have been reported, in a preliminary way, though.[8-10]

In this paper we report the luminescence of the Eu^{3+}-doped low-pressure form of the disilicates C-$M_2Si_2O_7$ (M = Y, Lu, Sc, as well as In). As a result of the analysis of the luminescence spectra recorded at 77 and 300 K under u.v. radiation the ^7F_J (J = 0—5) level schemes could be derived for all Eu^{3+}-doped C-$M_2Si_2O_7$. The energy-level schemes were used to obtain the even-rank crystal-field (c.f.) parameters with the aid of the phenomenological c.f. theory. The results of the c.f. simulation were compared to those obtained for the other Eu^{3+}-doped rare-earth-metal compounds.[11-19]

Experimental

Preparation of Samples.—The polycrystalline $M_2Si_2O_7$ (M = Y, Lu, Sc, or In) samples were prepared by the direct reaction between the rare-earth-metal oxide and amorphous silicon oxide (in 1:2 molar ratio) in air. Reaction temperatures between 1 520 and 1 620 K were employed in order to force the reaction to completion. A typical firing time used was between 60 and 180 h. The long firing times indicate that the reaction between the rare-earth-metal and silicon oxides occurs very slowly involving probably slow diffusion. Routine X-ray powder diffraction analysis of the products revealed the absence of other phases with the exception of the scandium compound. This impurity phase was identified as a high-temperature form of

scandium oxide, Sc_2O_3. All of the samples were doped with the Eu^{3+} ion (nominally 5 mol%).

Optical Measurements.—The luminescence of the $M_2Si_2O_7$ powder samples doped with the Eu^{3+} ion was measured under both u.v. and dye-laser excitation at 300 and 77 K. The radiation from a 200-W mercury lamp was centred with wide-band filters around 300 nm to correspond to the strongly absorbing charge-transfer band of Eu^{3+} ion in $M_2Si_2O_7$.

In order to avoid the luminescence of the impurity phases a Spectra Physics 375/376 continuous-wave rhodamine 6G dye laser (linewidth 0.7 cm^{-1}) pumped by a Spectra Physics 164 continuous-wave argon-ion laser was used to excite selectively the lowest excited ^5D level, $^5D_0$, near 580 nm. Luminescence was dispersed by a 1-m Jarrell-Ash Cerny-Turner type monochromator and was detected by a Hamamatsu R374 photomultiplier. The resolution of the equipment was better than 1.0 cm^{-1}. The $^5D_0 \rightarrow {}^7F_{0-5}$ transitions between 575 and 775 nm were considered in detail.

Crystal Structure.—The disilicate composition (with the $M_2O_3:SiO_2$ ratio 1:2) is known for the whole rare-earth-metal series. Despite the same composition the structure of the disilicates varies nearly from one rare earth metal to another. As much as seven different polymorphic forms have been found.[2] The heavier rare earths (including yttrium and scandium) yield only one stable form under ambient pressure, however. The stable rare-earth-metal disilicate, C-$M_2Si_2O_7$, possesses the thortveitite type structure. The C-$M_2Si_2O_7$ disilicates from holmium to lutetium crystallize in the monoclinic crystal system with $C2/m$ as the space group (Z = 2).[2]

A detailed crystal-structure determination has been given for both $Sc_2Si_2O_7$[20,21] and $Yb_2Si_2O_7$.[22] The crystal structure consists of the Si_2O_7 double tetrahedra as well as of the MO_6 octahedra. The two SiO_4 tetrahedra within the $Si_2O_7{}^{6-}$ group are linked with an angle of 180°. According to the structural data the rare-earth-metal ions occupy one crystallographically equivalent site with C_2 symmetry. The distortions from the ideal symmetry within the MO_6 octahedron are only of

Table 1. Energies (cm⁻¹) of the $^5D_0 \rightarrow {}^7F_{0-5}$ transitions observed in the emission spectrum of Eu³⁺-doped $M_2Si_2O_7$

Transition	M			
	Sc	In	Lu	Y
$^5D_0 \rightarrow {}^7F_0$	17 244	17 247	17 250	17 253
$^5D_0 \rightarrow {}^7F_1$	17 015	17 030	17 033	17 033
	16 898	16 878	16 863	16 858
	16 672	16 697	16 731	16 748
$^5D_0 \rightarrow {}^7F_2$	16 359	16 364	16 372	16 375
	16 321	16 324	16 316	16 321
	16 163	16 184	16 172	16 171
		16 137		
	15 939	15 939	15 972	15 980
$^5D_0 \rightarrow {}^7F_3$	15 422	15 415		
	15 340	15 356	15 363	15 368
	15 295	15 330	15 323	15 321
		15 295	15 284	15 286
	15 216	15 232	15 242	15 249
	15 198	15 207	15 216	15 235
	15 101	15 110	15 135	15 145
$^5D_0 \rightarrow {}^7F_4$	14 548	14 554	14 554	14 556
	14 522	14 526	14 524	14 524
	14 411	14 415	14 463	14 484
	14 292	14 292	14 263	14 255
	14 217	14 219	14 215	14 215
	14 184	14 180	14 164	14 174
	14 128	14 134	14 136	
	14 086	14 098	14 124	14 140
		14 088	14 106	14 110
$^5D_0 \rightarrow {}^7F_5$	13 492	13 499		
	13 470		13 490	13 486
	13 399	13 410	13 405	13 403
	13 382		13 376	13 385
		13 316	13 317	13 319
	13 308	13 217		
	13 215		13 259	13 273
	13 180	13 184	13 198	13 212
	13 034	13 034	13 038	
			13 014	13 015
	12 981	12 952	12 972	12 982

minor importance as the following scandium–oxygen distances show: 2.083, 2.100, and 2.189 Å.[20]

Results and Discussion

Analysis of the Luminescence Spectra.—The Eu³⁺-doped $M_2Si_2O_7$ powder samples yield reddish luminescence under u.v. excitation. The emission originates from the electronic transitions from the lowest level, $^5D_0$, of the first excited multiplet, ^5D, to the ground septet, ^7F_J ($J = 0$—6).[23] No emission from the higher excited levels, e.g. $^5D_{1-4}$, was observed. The absence of the $^5D_{1-4} \rightarrow {}^7F_J$ emission is most probably caused by the multiphonon de-excitation of the excitation energy. Despite the relatively high concentration of the dopant (5 mol %), concentration quenching effects can be ruled out.

The low point symmetry of the rare-earth-metal site allows the magnetic dipole (m.d.) as well as the electric dipole (e.d.) induced transitions (Table 1). Consequently, the $^5D_0 \rightarrow {}^7F_1$ m.d. transitions have intensities equal to those of the e.d. transitions, $^5D_0 \rightarrow {}^7F_2$ and $^5D_0 \rightarrow {}^7F_4$ (Figure 1). In addition to the pure m.d. and e.d. transitions also the $^5D_0 \rightarrow {}^7F_3$ and $^5D_0 \rightarrow {}^7F_5$ transitions have non-negligible intensity due
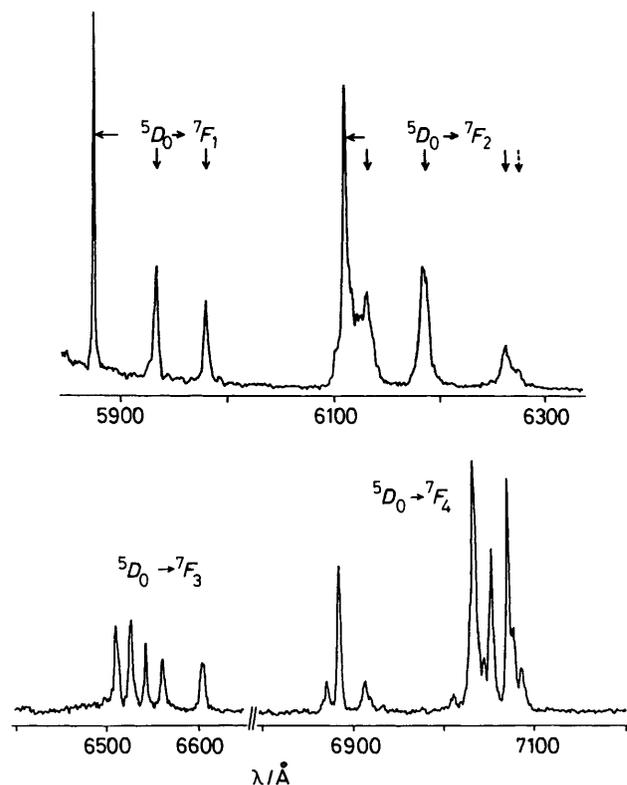
Figure 1. Part of the visible luminescence spectrum of Eu³⁺-doped $Lu_2Si_2O_7$ at 77 K under rhodamine 6G dye-laser excitation

to the mixing of the $^7F_{JM}$ ($J = 3$ or 5) wavefunctions with the $^7F_{2,4,6}$ ones.[24] The $^5D_0 \rightarrow {}^7F_0$ transition has a low intensity in the $M_2Si_2O_7$ matrices. Group theory allows this transition for the C_n, C_s, and C_{nv} site symmetries.[25] The intensity of the $^5D_0 \rightarrow {}^7F_0$ transition depends on the one hand on the linear odd-rank c.f. term A_0^1 and on the other on the amount of the contributions of the $^7F_{JM}$ ($J = 2$ or 4) wavefunctions with the $^7F_{00}$ one. The number of lines in the c.f. fine structure of the emission spectra reveals a total of $2J + 1$ lines for each $^5D_0 \rightarrow {}^7F_J$ transition. This observation is in accordance with the C_2 site symmetry which lifts completely the total angular momentum degeneracy of the ^7F_J energy levels. There exist no valid selection rules, either, for the site symmetries lower than C_{2v} which would restrict the number of emission lines to be observed experimentally.

The $^7F_{JM}$ energy-level schemes derived from the emission spectra are rather similar in all $M_2Si_2O_7$ matrices studied. The schemes are characterized by relatively strong splittings of the ^7F_J levels (Table 2). Though the structural data suggest only slight deviations in the M–O distances from the ideal octahedral co-ordination, the optical data give no support to this assumption since no 'pseudo-doublets' can be observed in the $^7F_{JM}$ schemes. Furthermore, the presence of the intense electric dipole transitions excludes the octahedral symmetry for the rare-earth-metal site. Despite the similarities in the energy-level schemes throughout the host cation series, a weak nephelauxetic effect can be observed in the energies of the excited levels (Table 2). The increase in the energy of the $^5D_0$ level along with the increasing radius of the host cation is in agreement with the general trend.[26]

Crystal-field Simulation of the $^7F_{0-5}$ Level Schemes.—Following Wybourne's formalism[27] the c.f. Hamiltonian can be expressed as a sum of the products between the real and imaginary c.f. parameters (B_q^k and S_q^k) and spherical harmonics (C_q^k) [equation (1)].

Table 2. Experimental and calculated $^7F_{0-5}$ energy-level schemes (in cm^{-1}) of Eu^{3+}-doped M$_2$Si$_2$O$_7$

		M							
		Sc		In		Lu		Y	
Level		exptl.	calc.	exptl.	calc.	exptl.	calc.	exptl.	calc.
$^7F_0$	A	0	0	0	0	0	0	0	0
$^7F_1$	B	229	226	217	210	217	217	220	219
	A	346	347	369	370	387	390	395	399
	B	572	575	550	557	519	517	505	505
$^7F_2$	B	885	880	883	890	878	876	878	883
	A	923	929	923	916	934	932	932	931
	A	1 081	1 078	1 063	1 062	1 078	1 082	1 082	1 080
	B		1 133	1 110	1 109		1 106		1 111
	A	1 305	1 309	1 308	1 311	1 278	1 277	1 273	1 275
$^7F_3$	B	1 822	1 823	1 832	1 830		1 841		1 842
	A	1 904	1 908	1 891	1 897	1 887	1 891	1 885	1 890
	B	1 949	1 953	1 917	1 920	1 927	1 929	1 932	1 931
	A		1 968	1 952	1 952	1 966	1 963	1 967	1 962
	B	2 028	2 032	2 015	2 010	2 008	2 019	2 004	2 008
	A	2 046	2 044	2 040	2 041	2 034	2 028	2 018	2 022
	B	2 143	2 134	2 137	2 136	2 115	2 110	2 108	2 103
$^7F_4$	A	2 696	2 688	2 693	2 691	2 696	2 695	2 697	2 698
	B	2 722	2 725	2 721	2 720	2 726	2 729	2 729	2 731
	A	2 833	2 835	2 832	2 826	2 787	2 779	2 769	2 766
	A	2 952	2 960	2 955	2 954	2 987	2 985	2 998	2 995
	B	3 027	3 027	3 028	3 035	3 035	3 036	3 038	3 034
	A	3 060	3 058	3 067	3 068	3 086	3 087	3 079	3 083
	A	3 116	3 116	3 113	3 112	3 114	3 112		3 105
	B	3 158	3 157	3 149	3 147	3 126	3 126	3 113	3 116
	B		3 198	3 159	3 165	3 144	3 152	3 143	3 145
$^7F_5$	A	3 752	3 756	3 748			3 747		3 753
	B	3 775	3 770		3 766	3 760	3 757	3 767	3 766
	A	3 845	3 844	3 837	3 841	3 845	3 850	3 850	3 850
	B	3 862	3 867		3 929	3 874	3 865	3 868	3 866
	B		3 901	3 932	3 931	3 933	3 931	3 934	3 931
	A	3 936	3 936	4 030	4 029		3 963		3 960
	B	4 029	4 028		4 034	3 991	3 991	3 980	3 981
	A	4 064	4 066	4 063	4 065	4 052	4 056	4 041	4 041
	A	4 210	4 205	4 213	4 213	4 212	4 217		4 227
	B	4 263	4 266		4 223	4 236	4 240	4 238	4 241
	B		4 320	4 295	4 292	4 278	4 272	4 271	4 271
$^5D_0$	A	17 244		17 247		17 250		17 253	

$$H_{cf} = \sum_{kq}[B_q^k(C_q^k + C_{-q}^k) + iS_q^k(C_q^k - C_{-q}^k)] \quad (1)$$

The C_2 symmetry induces a c.f. Hamiltonian $[H_{cf}(C_2)]$ which contains as much as 14 parameters (including five imaginary ones). The final c.f. Hamiltonian used to fit experimentally observed $^7F_{0-5}$ level schemes is as in equation (2).

$$\begin{aligned}
H_{cf}(C_2) = & B_0^2 C_0^2 + B_0^4 C_0^4 + B_0^6 C_0^6 + B_2^2(C_2^2 \\
& + C_{-2}^2) + B_2^4(C_2^4 + C_{-2}^4) + B_2^6(C_2^6 \\
& + C_{-2}^6) + B_4^4(C_4^4 + C_{-4}^4) + B_4^6(C_4^6 \\
& + C_{-4}^6) + B_6^6(C_6^6 + C_{-6}^6) + S_2^4(C_2^4 - C_{-2}^4) \\
& + S_2^6(C_2^6 - C_{-2}^6) + S_4^4(C_4^4 - C_{-4}^4) \\
& + S_4^6(C_4^6 - C_{-4}^6) + S_6^6(C_6^6 - C_{-6}^6)
\end{aligned} \quad (2)$$

The actual simulation of the experimental $^7F_{0-5}$ energy-level schemes was carried out by minimizing the root mean square (r.m.s.) deviations between the experimental and calculated level schemes with the aid of a matrix diagonalization and least-squares refinement program IMAGE.[28] The starting values for the crystal-field parameters were obtained by modified lattice-sum calculations taking into account the effective charge and distance of the ions.

The phenomenological simulation of the c.f. splittings between the 30 to 32 Stark levels of the ^7F_J energy levels yielded excellent results. The overall r.m.s. deviation between the calculated and experimental energy levels varies between 4 and 6 cm^{-1} (Table 3). Furthermore, no individual discrepancies within the energy-level schemes can be observed (Figure 2).

The best-fit sets of the B_q^k and S_q^k parameters are characterized by a weak B_0^2 and a strong B_2^2 parameter. The high value of the B_2^2 parameter indicates an important deviation from higher symmetry than the C_{2v} one for the rare-earth-metal site. When this result is compared to the slight differences in rare-earth-metal–oxygen distances given by the structural data it is evident that even slight distortions induce significant effects in the crystal field experienced by the M^{3+} ion. A significant distortion even from the C_{2v} symmetry is revealed by the unusually strong S_2^4 parameter.

Table 3. The values of the even-rank c.f. parameters (all values in cm⁻¹) for Eu^{3+}-doped $M_2Si_2O_7$. The numbers in parentheses are the standard deviations

B_q^k	M Sc	In	Lu	Y
B_0^2	−277(22)	−127(23)	40(21)	95(24)
B_2^2	−905(15)	−867(17)	−755(12)	−716(18)
B_0^4	−901(55)	−1 042(42)	−1 092(51)	−1 047(46)
B_2^4	−403(28)	−627(24)	−318(23)	−350(23)
S_2^4	−1 606(36)	−1 360(27)	−1 541(29)	−1 555(24)
B_4^4	−652(22)	−483(21)	−567(21)	−571(24)
S_4^4	100(25)	474(25)	154(23)	156(19)
B_0^6	−1 208(45)	−462(70)	−994(55)	−964(78)
B_2^6	143(40)	347(39)	−13(28)	−2(38)
S_2^6	417(44)	25(37)	198(39)	166(27)
B_4^6	202(35)	179(34)	−91(29)	−147(24)
S_4^6	65(35)	259(34)	488(29)	448(29)
B_6^6	−242(34)	−118(28)	54(28)	−13(32)
S_6^6	213(39)	−557(29)	−425(28)	−431(23)
S	659	612	615	608
R.m.s. deviation	5.4	4.9	5.8	3.8
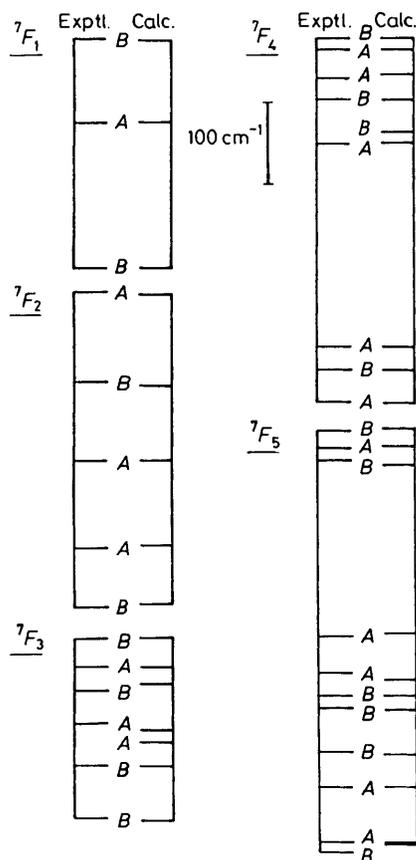
Figure 2. Comparison between the calculated and experimental c.f. splittings of $^7F_{0-5}$ levels of Eu^{3+}-doped $Y_2Si_2O_7$

As a consequence of the rather similar $^7F_{0-5}$ energy-level schemes the c.f. parameter sets obtained for the $M_2Si_2O_7$ (M = Y, Lu, In, or Sc) series resemble one another. The evolution of the parameter values throughout the whole series is quite smooth. However, the best-fit parameter set obtained for the $In_2Si_2O_7$ host is an exception to this smooth behaviour. This exception is comprehensible since, despite the apparent similarities of the indium compounds to the rare-earth-metal

systems, basically indium differs from the rare-earth group. The c.f. effect (monitored as the value of the c.f. strength parameter S,[29] Table 3) increases slightly with decreasing ionic radius of the host cation. Similar behaviour has been encountered in most isomorphic rare-earth-metal compound series, e.g. in oxide sulphates,[17] oxide hydroxides,[30,31] and oxide sulphides.[18] This may be an indication of the importance of the ionic contribution in the bonding between the rare-earth metal and oxygen atoms since electrostatic point-charge calculations have shown such a behaviour in the oxide halide series.[32]

The comparison of the emission spectra and the $^7F_{0-5}$ energy-level schemes of Eu^{3+}-doped $C-M_2Si_2O_7$ reveal significant differences from those of the typical rare-earth-metal oxysalts. Despite the similarity of the empirical formulae, the structural data indicate the absence of the structural units typical of the oxysalts, i.e. the OM_4 tetrahedra,[33,34] in the structure of disilicates. This dissimilarity is confirmed by the fundamental differences in the c.f. parameter sets. As a consequence of both the structural and spectroscopic data it must be concluded that, despite the similarity of the empirical chemical formulae, the rare-earth-metal disilicates do not belong to the family of oxy compounds.

References

1 H. Strunz, 'Mineralogische Tabellen,' 5th edn., Akademische Verlagsgesellschaft, Leipzig, 1970, p. 621.
2 J. Felche, Struct. Bonding (Berlin), 1973, 13, 99.
3 G. Bocquillon, C. Loriers-Susse, M. Dellalian, and J. Loriers, C.R. Acad. Sci., Ser. C, 1973, 276, 543.
4 J. Felche, J. Less-Common Met., 1970, 21, 1.
5 G. Bocquillon, C. Chateau, C. Loriers, and J. Loriers, J. Solid State Chem., 1977, 20, 135.
6 J. Loriers, G. Bocquillon, C. Chateau, and D. Colaitis, Mater. Res. Bull., 1977, 12, 403.
7 C. Chateau and J. Loriers, C.R. Acad. Sci., Ser. C, 1979, 288, 421.
8 G. Bocquillon, C. Chateau, and J. Loriers, in 'Rare Earths in Modern Science and Technology,' eds. G. S. McCarthy, J. J. Rhyne, and H. B. Silber, Plenum, New York, 1980, p. 209.
9 F. Bretheau-Raynal, N. Tercier, B. Blanzat, and M. Drifford, Mater. Res. Bull., 1980, 15, 639.
10 Y. Tsujimoto, Y. Fukuda, S. Sugai, and M. Fukai, J. Lumin., 1975, 9, 475.
11 J. Hölsä, K. Jyrkäs, and M. Leskelä, J. Less-Common Met., 1986, 126, 215.
12 J. Hölsä and P. Porcher, J. Chem. Phys., 1982, 76, 2798.
13 J. Hölsä and P. Porcher, J. Less-Common Met., 1985, 112, 127.
14 J. Huang, J. Loriers, and P. Porcher, J. Solid State Chem., 1982, 43, 87.
15 O-K. Moune-Minn and P. Caro, J. Crystallogr. Spectrosc. Res., 1982, 12, 157.
16 J. Hölsä and P. Porcher, J. Chem. Phys., 1981, 75, 2108.
17 P. Porcher, D. R. Svoronos, M. Leskelä, and J. Hölsä, J. Solid State Chem., 1983, 46, 101.
18 O. J. Sovers and T. Yoshioka, J. Chem. Phys., 1969, 51, 5330.
19 J. Hölsä, T. Leskelä, and M. Leskelä, Inorg. Chem., 1985, 24, 1539.
20 Y. U. Smolin, Y. U. Shepelev, and A. P. Titov, Sov. Phys. Crystallogr. (Engl. Transl.), 1973, 17, 749.
21 D. W. J. Cruickshank, H. Lynton, and G. A. Barclay, Acta Crystallogr., 1962, 15, 491.
22 Y. U. Smolin and Y. U. Shepelev, Acta Crystallogr., Sect. B, 1970, 26, 484.
23 G. H. Dieke, 'Spectra and Energy Levels of Rare Earth Ions in Crystals,' Interscience, New York, 1968.
24 P. Porcher and P. Caro, J. Lumin., 1980, 21, 207.
25 G. Blasse, Struct. Bonding (Berlin), 1976, 26, 43.
26 P. Caro, O. Beaury, and E. Antic, J. Phys. (Paris), 1976, 37, 671.

27 B. G. Wybourne, 'Spectroscopic Properties of Ions in Crystals,' Interscience, New York, 1965.

28 P. Porcher, unpublished work.

29 N. C. Chang, J. B. Gruber, R. P. Leavitt, and C. A. Morrison, *J. Chem. Phys.*, 1982, **76**, 3877.

30 J. Hölsä, *J. Phys. Chem.*, in the press.

31 J. Hölsä, *Z. Naturforsch.*, in the press.

32 J. Hölsä, *Ann. Acad. Sci. Fenn., Ser. A2*, 1983, **196**, 1.

33 P. Caro, *C.R. Acad. Sci., Ser. C*, 1966, **262**, 992.

34 P. Caro, *J. Less-Common Met.*, 1968, **16**, 367.